# Studies on multipass welding with trailing heat sink considering phase transformation

Shirish R. Kala [a], N. Siva Prasad [a,*], G. Phanikumar [b]

[a] Department of Mechanical Engineering, Indian Institute of Technology Madras, Chennai 600036, India
[b] Department of Metallurgical and Materials Engineering, Indian Institute of Technology Madras, Chennai 600036, India

## ABSTRACT

A two pass butt welding of 6 mm mild steel plates was simulated using 3D finite element model using temperature and phase dependent material properties. Material phase transformations were simulated using suitable phase transformation kinetic models. Mechanical analysis is carried out using nodal temperature and phase proportions as input. Experiments were carried out using liquid nitrogen (LN2) as trailing heat sink. Trailing heat sink helped to reduce the residual stress in the fusion zone (FZ) and heat affected zone (HAZ) although distortions were found be increasing. A parametric study was conducted to study the effect of distance between weld arc and trailing heat sink. The heat sink closer to weld arc reduced both distortions and residual stresses.

© 2014 Published by Elsevier B.V.

## 1. Introduction

Fusion welding is an effective metal joining process extensively used in fabrication of structures. The nonuniform and localized heating results into weld distortions and residual stresses. Finite element modelling (FEM) is an effective tool which can be used to predict the distortion and residual stresses in the welded joints.

Li et al. (2004) investigated TIG welding both numerically and experimentally for titanium alloy using conventional welding and modified process in which trailing heat sink was introduced to control residual stresses and distortion. van der Aa et al. (2006b) used a five bar conceptual model to explain development of longitudinal plastic strain and stress during conventional welding and compared it with welding with trailing heat sink. The model demonstrated that modified temperature profile results into changes in thermal strains in the bars causing increased stress in one bar which was balanced by decrease in stress in other bars.

Yanagida and Koide (2008) carried out multipass welding with trailing water shower and different interpass time. They found that by applying water shower with suitable interpass time the tensile residual stresses were converted to compressive residual stress

which is good to prevent stress corrosion cracking. Sudheesh and Siva Prasad (2011) studied the effect of liquid nitrogen trailing heat sink on distortion and residual stresses in single pass arc welding. The introduction of liquid nitrogen reduced residual stress and distortion by redistributing thermal strains and distortion.

Soul and Yanhua (2005) demonstrated through numerical studies that welding with trailing sink reduced residual stresses and minimized distortion in thin plates. van der Aa et al. (2006a) found that active cooling in the form of trailing heat sink reduces the negative transverse stresses below critical buckling stress and hence eliminated the buckling distortion.

Heinze et al. (2012) conducted numerical and experimental investigation on the effect of transverse shrinkage in multipass welding. Transverse shrinkage was imposed in order to include actual structural effects. Deng and Murakawa (2008) developed computational procedure to calculate temperature field, microstructure and residual stresses in multipass butt welded joint of 2.25Cr-1Mo steel pipes, considering the influence of solid state phase transformation. It was suggested that phase dependent material properties must be incorporated in the analysis to obtain accurate results.

Borjesson and Lindgren (2001) simulated multipass welding using temperature and phase dependent material properties where properties of individual phases were subjected to mixture rule to calculate the macro material property. Residual stresses measured using hole drilling technique showed good agreement with

* Corresponding author. Tel.: +91 44 22574679; fax: +91 44 22574652.
*E-mail addresses:* shirishkala@yahoo.com (S.R. Kala), siva@iitm.ac.in
(N. Siva Prasad), gphani@iitm.ac.in (G. Phanikumar).

calculated residual stresses in transverse direction but not in longitudinal direction.

Lee and Chang (2009) conducted finite element analysis of high carbon steel multipass butt weld considering solid state phase transformation. It was concluded that volumetric increase during austenite to martensite phase transformation reduced longitudinal tensile residual stresses in the weld region and heat affected zone. Becker et al. (2005) attempted to predict phase transformation, phase dependent material properties and residual stresses using experimentally determined continuously cooling transformation (CCT) diagrams.

Wang and Felicelli (2007) developed a three dimensional finite element model to predict the temperature distribution and phase transformation in laser deposition process. They calculated molten pool size and volume fraction of solid phases formed at different speeds. Deng (2009) noted that in medium carbon steel, the solid state phase transformation has significant effect on residual stresses and distortion values due to large dilatation and low transformation temperature, whereas for low carbon steel, phase transformation has no significant effect on calculated values because of small dilatation and relatively high temperature range.

Ferro et al. (2006) investigated the effect of phase transformation considering both volume change and transformation plasticity on residual stress calculation using 2D and 3D numerical models. Han et al. (2011) developed constitutive models for elasto-plastic deformation which included transformation plasticity and Leblonde's phase evolution equation (Leblond and Devaux, 1984). They demonstrated that the phase transformation and transformation plasticity had significant effect on residual stresses of a welded structure.

In the present study a multipass welding of mild steel plates was numerically simulated for conventional welding and welding with trailing heat sink using commercial finite element software Sysweld. The results were validated with experiments using liquid nitrogen (LN2) jet as trailing heat sink. Effect of phase transformations was studied by conducting numerical simulation with and without phase transformations. Preliminary trials on multipass welding with heat sink showed an increase in distortion. In
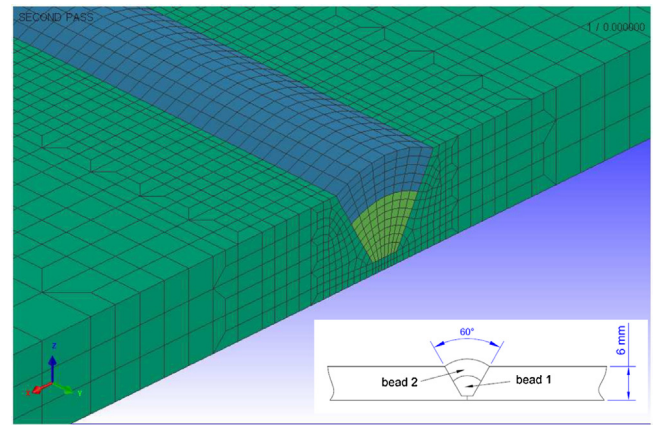


**Fig. 1.** Mesh of two pass butt joint.

this study, the role of distance between heat sink and heat source on the magnitude of distortion during multipass welds is demonstrated.

## 2. Finite element analysis (FEA)

A 3D finite element mesh of two mild steel plates of size 300 mm × 75 mm × 6 mm is shown in Fig. 1. The V-groove of weld cross-section is shown in the inset of Fig. 1. The weld zone and expected heat zone is modelled with smaller brick elements of better aspect ratio. The region away from weld line are meshed coarsely and penta elements are used as transition elements between fine and coarse mesh. The meshed model consists of 119,400 solid elements to represent plate material, 24,904 2D elements on the surface of the plate to facilitate convection heat loss from plate material to the atmosphere. In addition, there are 600 1D elements to model weld path for two weld passes. Weld passes are modelled with a set of elements grouped separately and designated as *bead1* and *bead2*. A group of three nodes on the back of the plate are used to assign minimum clamping condition which would arrest the rigid body motions. The thermo-metallurgical analysis is conducted to calculate the transient temperature distribution and phase proportion which is followed by mechanical analysis to determine distortions and residual stresses in the welded plates.

### 2.1. Material modelling

Numerical simulation of welding process involves computation of transient temperature distribution and its effect on stress and strain and in turn on the material geometry. Temperature dependent thermal and structural properties of the material are required as temperatures are expected to vary from room temperature to above melting temperature. Analysis which includes phase transformations require material properties for various phases which the material may undergo. Material considered in this study is mild steel. As the material is heated, initial phase ferrite or bainite is transformed to austenite and during cooling austenite is transformed to bainite, martensite or ferrite depending upon the cooling rate. Accurate prediction of distortions and residual stresses during welding require material properties for all the phases as a function of temperature. A set of cooling rates extracted from the continuous cooling transformation (CCT) diagram are provided in the material database. Various thermal properties considered are specific heat, thermal conductivity and density and structural properties are Young's modulus, thermal strain, Poisson's ratio, yield strength and strain hardening data. The material properties used are also available in Heinze et al. (2012). The analysis without phase
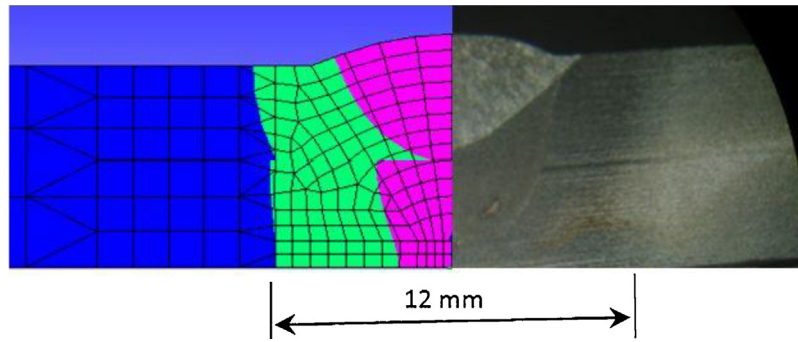
**Fig. 2.** Heat source fitting.

transformation is carried out using properties of only ferritic phase of the material.

## 2.2. Thermal analysis

The moving heat source is modelled using Goldak (Goldak et al., 1984) double ellipsoidal model (Eqs. (1) and (2)) as the process assumed here is tungsten inert gas (TIG) welding which is a slow speed process and double ellipsoidal model is most suitable for it.

$$Q_f(x, \xi, z) = \frac{6\sqrt{3}Q}{ab_f c\pi\sqrt{\pi}} \exp\left(-3\frac{x^2}{a^2} - 3\frac{\xi^2}{b_f^2} - 3\frac{z^2}{c^2}\right) \tag{1}$$

$$Q_r(x, \xi, z) = \frac{6\sqrt{3}Q}{ab_r c\pi\sqrt{\pi}} \exp\left(-3\frac{x^2}{a^2} - 3\frac{\xi^2}{b_r^2} - 3\frac{z^2}{c^2}\right) \tag{2}$$

where net heat input $Q = \eta VI$ and $\xi = y - v(\varsigma - t)\eta = 65\%$ (assumed), $V = 10$ V, $I = 170$ Å.

The following Goldak parameters assumed in this study are $a = 4$ mm, $b_f = 4$ mm; $b_r = 5$ mm; and $c = 3$ mm. The values of $Q_f$ and $Q_r$ are front and rear heat source intensity in W/mm$^3$, are calculated using net heat input $Q$ and adjusted in proportion along with other parameters to match with the size and shape of molten zone. Fig. 2 shows a comparison between calculated and experimentally determined size and shape of fusion and heat affected zone.

Cooling flux is modelled using Gaussian distribution by Eq. (3), applied to the thermal model at a fixed distance behind the weld arc. Negative cooling flux is assumed and adjusted so as to match with the experimental temperature profile for a cooling jet of radius $\bar{r} = 2.5$ mm. Temperature distribution at a given time instance

shown in Fig. 3 indicates the heat source by a peak and heat sink by the trough in the graph.

$$q(x, y, r) = \frac{3Q}{\pi\bar{r}^2} \exp\left(-3\left(\frac{r}{\bar{r}}\right)^2\right) \tag{3}$$

where

$$r^2 = (x - x_o)^2 + (y - y_o - vt)^2$$

The governing differential equation for heat conduction without heat generation is given in Eq.(4).

$$\frac{\partial}{\partial(x)}\left[k_x \frac{\partial T}{\partial x}\right] + \frac{\partial}{\partial(y)}\left[k_y \frac{\partial T}{\partial x}\right] + \frac{\partial}{\partial(z)}\left[k_z \frac{\partial T}{\partial x}\right] + q_{sup} = \rho c \frac{\partial T}{\partial t} \tag{4}$$

In addition to heat source and trailing heat sink which are moving boundary conditions, the initial nodal temperature is assumed to be ambient temperature and effective convective heat transfer which includes radiation losses, is applied over the entire outer boundary of the model.

## 2.3. Phase transformation

The solid state phase transformation effects are considered by including the phase dependent material properties as well as phase transformation kinetic models. The diffusion based phase transformations such as austenite to bainite/ferrite are modelled using Leblond model (Leblond and Devaux, 1984) as given in Eq. (5). The diffusion less transformation such as austenite to martensite is modelled using Koinstinen Marburger model (Koistinen and
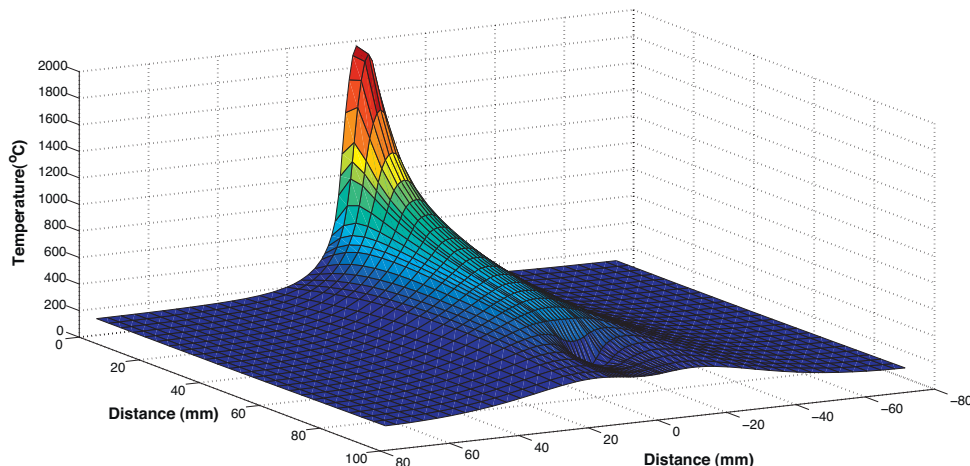


**Fig. 3.** Heat source and trailing heat sink.

Marburger, 1959) as given in Eq. (6). The kinetic model parameters are extracted from the CCT diagram of the given material.

$$\frac{dP(T)}{dt} = f(\dot{T})\frac{P_{eq}(T) - P(T)}{\tau(T)} \tag{5}$$

$$P(T) = 1 - \exp(-b(M_s - T)) \tag{6}$$

Element activation of filler or bead materials is achieved by phase transformation procedure using *chewing gum method* (Sysweld, 2005). During the welding of first pass when a heat source is moved along the elements of first bead, elements of second bead are assumed to be *dummy material*. Dummy material has a low thermal conductivity and elasticity, hence, they do not contribute in numerical calculations. Since second bead does not exist during the welding of first bead, the elements of second bead expands or contract the way chewing gum would due to its low elasticity. Elements of first bead during welding of first pass are modelled as a material of base plate but with *dummy phase*. As material is assumed to have multiple phases, one of the phase can be assumed as dummy phase which is assigned to the elements of first bead. Phase transformation reaction for the dummy phase is defined such that when the nodal temperature of these elements exceeds the melting temperature of the base material, dummy phase gets transformed to austenite and then to subsequent phases depending upon its cooling rate.

### 2.4. Mechanical analysis

Residual stresses in multiphase material such as steel arise due to difference in thermal expansion, yield stress and stiffness of different phases in addition to temperature gradient (Dai et al., 2008). The FE analysis carried out is sequentially coupled, thermo-metallurgical followed by mechanical analysis. Nodal temperature and phase proportion values computed in thermo-metallurgical analysis are taken as input to the mechanical analysis. A law of linear weighting as a function phase proportion is used for ferritic mixture as given in Eq. (7) and nonlinear weighting function is used for austeno-ferritic mixtue as given in Eq. (8).

$$\sigma_y^\alpha(\theta) = \sum P_i \sigma_i^\alpha(\theta) \tag{7}$$

$$\sigma_y^\alpha(\theta) = [1 - f(\lambda)]\sigma_i^\gamma(\theta) + f(\lambda)\sigma_i^\alpha(\theta) \tag{8}$$

Similarly, thermal strain due to metallurgical factors is expressed as given in Eq. (9).

$$\varepsilon^{th}(P, \theta) = \sum P_i \varepsilon_i^{th}(\theta) \tag{9}$$

Thermal stain values are provided for both austenite and ferrite phases. Transformation plasticity which is occurrence of plastic flow of weaker phases even below yield stress due to the presence of stronger phase is also included. The total strain rate is given by the following equation.

$$\dot{\varepsilon} = \dot{\varepsilon}^e + \dot{\varepsilon}^{th} + \dot{\varepsilon}^{pc} + \dot{\varepsilon}^{tp} \tag{10}$$

Mechanical analysis is carried out by considering geometric nonlinearity and stain hardening is assumed to be isotropic. The minimum mechanical constraints are applied to avoid rigid body motion. Three corner nodes on the base of the plate are constrained such that first node is arrested in $x, y, z$ direction, second node in $x, z$ direction and the third node in only $z$ direction, effectively arresting six degrees of freedom.

## 3. Experimentation

An experimental setup has been developed as shown in Fig. 4. A liquid nitrogen (LN2) jet nozzle is attached to a TIG welding torch.
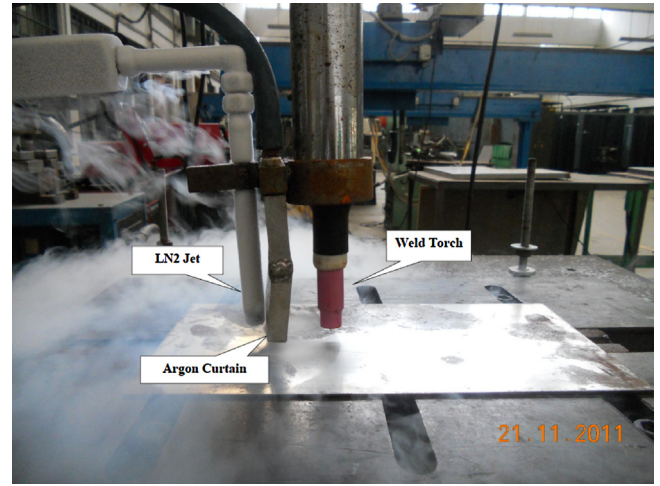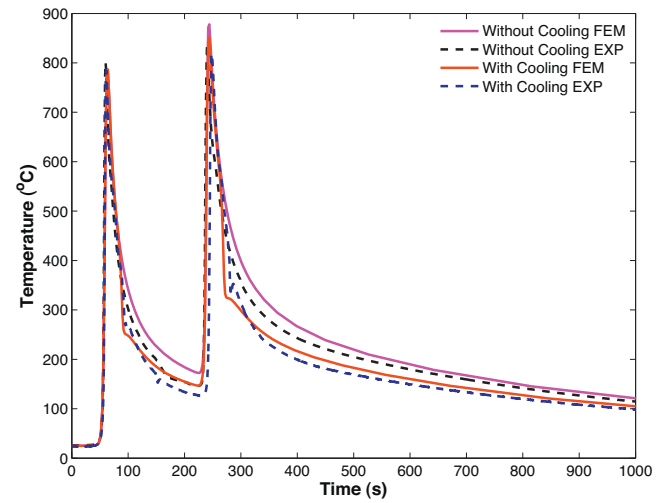


**Fig. 4.** Experimental setup.



**Fig. 5.** Thermal profile experienced at a location 5 mm away from weld centerline.

The liquid nitrogen container (Dewar) is attached with nitrogen gas to pressurize and pump liquid out. The LN2 container is provided with a tightly closed lid which helps to build pressure inside the container. An insulated flexible hose is used to transfer LN2 from the pipe to the workpiece surface through a nozzle. A valve is provided at the outlet to control the flow.
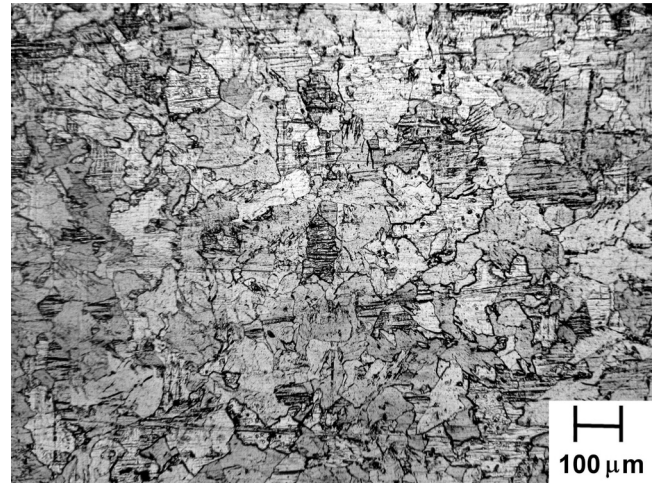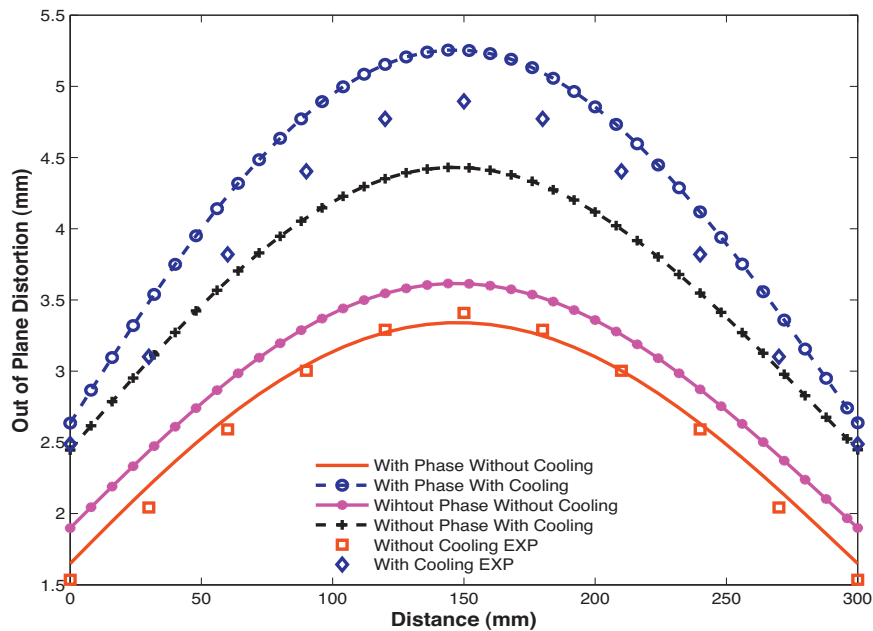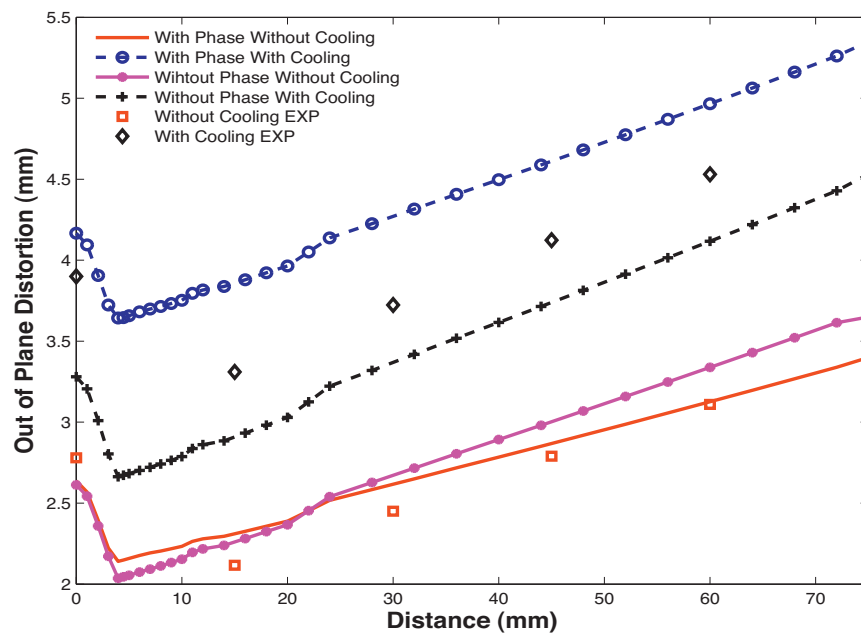


**Fig. 6.** Mixed phases in weld bead.

(a) Longitudinal direction



(b) Transverse direction

**Fig. 7.** Out of plane distortion.

The liquid nitrogen after jetting rapidly turns into nitrogen gas which disturbs the weld arc. To overcome this problem an argon gas curtain is inserted in between the weld torch and liquid nitrogen jet which prevent liquid or gas nitrogen moving towards the weld arc. As it can be noted from the experimental setup, the heat sink needs to be separated by a minimum distance (75 mm in this case) from the arc to accommodate argon curtain. Argon curtain prevents the liquid nitrogen entering into the arc without which a stable weld arc is not realizable in the current setup.

Experiments are conducted to validate the FEM results with an interpass time of 180 s. The plate edges are milled for 30° and 2 mm holes are drilled for fixing thermocouples. Two pass TIG welding is carried out with $V = 15$ V, $I = 170$ A, weld speed $v = 2.5$ mm/s and using filler wires of same material. The temperature values are measured at a point 5 mm away from weldline, on both sides of weld using k-type thermocouple and National Instruments (NI) data acquisition system (DAQ). The out of plane distortion is measured along free edge on plate in the longitudinal direction and along mid-length of plate in the transverse direction using dial-gauge indicator whose least count is 0.01 mm. The computed distortion values are generally symmetric and therefore in experimental measurements the datum is set to ensure this symmetry of distortion.
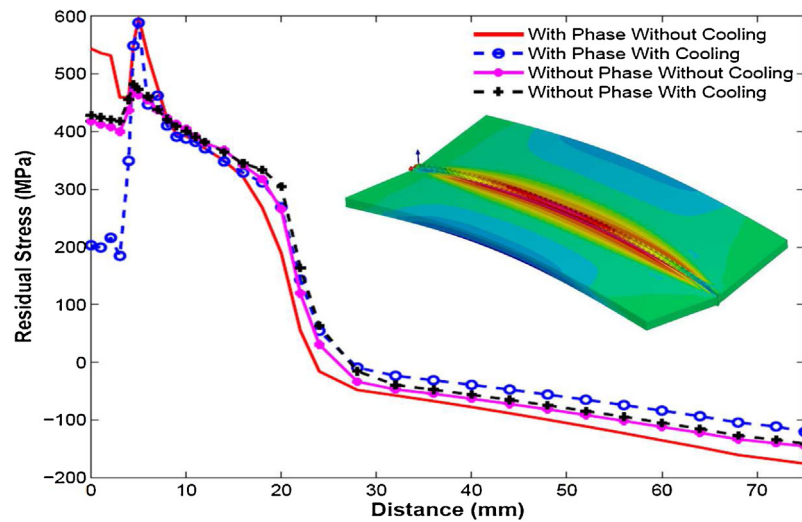
(a) Longitudinal residual stress
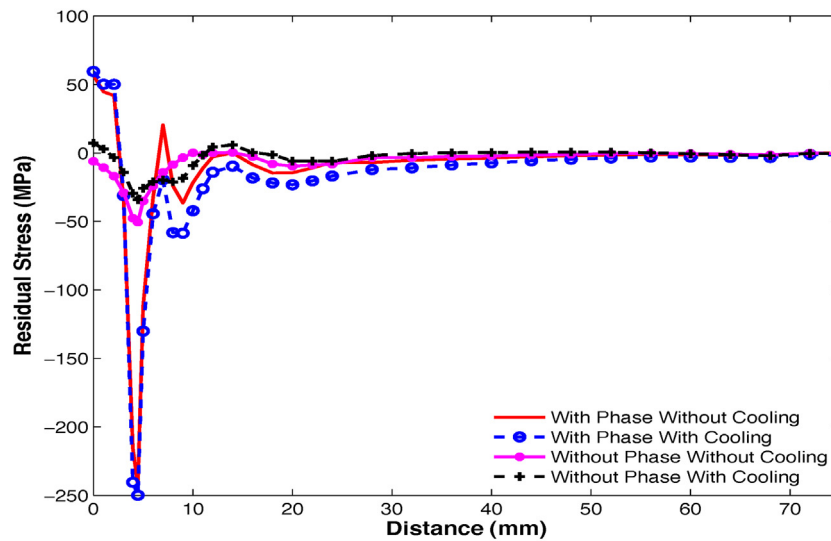


(b) Transverse residual stress

**Fig. 8.** Residual stresses.

## 4. Results and discussion

Fig. 5 shows the temperature measured at a distance 5 mm away from weldline. The temperature distribution with and without cooling both for experimentally measured and FEM simulated values are plotted. In case of with trailing heat sink, the cooling portion of curve is truncated due to rapid cooling. The trailing heat sink is applied at a distance 75 mm behind the heat source which is actual distance between weld torch and cooling jet in the experimental setup. Optical micrograph in Fig. 6 shows grains of two different contrasts that could be attributed to the mixture of two phases in the microstructure. The variation of bainite and martensite in both the beads for with and without cooling is given in Table 1. It can be observed that martensite proportion in both the beads is increased when welding is done with cooling. It can also be observed that the martensite proportion in second bead is less than first bead for welding without cooling and more when trailing heat sink is used. This is because in conventional welding last pass is cooled at a slower rate and receives less heat input than its previous passes. Whereas in welding with trailing heat sink, the

**Table 1**
Volume fraction of phases in %.

|  | Bainite | | Martensite | |
| --- | --- | --- | --- | --- |
|  | Bead1 | Bead2 | Bead1 | Bead2 |
| Without cooling | 84.1 | 95.9 | 15.7 | 3.9 |
| With cooling | 79.7 | 59.2 | 20.1 | 40.5 |

second pass undergoes more effective cooling as it is exposed to atmosphere.

Fig. 7(a) shows out of plane distortion measured along the free edge in the longitudinal direction which is 300 mm along length of the plate. Fig. 7(b) shows out of plane distortion measured along 75 mm width of the plate at mid section in the transverse direction along, which is perpendicular to weld line. It can be observed from the plots that distortions for without phase transformation case is less compared to phase transformations are considered. This is because in case of with phase transformations, the transformation plasticity is included which causes the additional strains which results in increased distortion. It can also be observed that
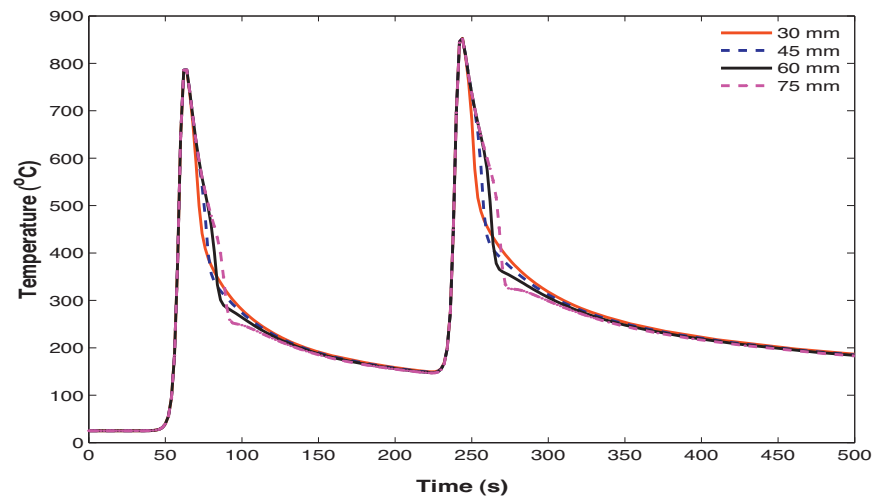
(a) Thermal profile
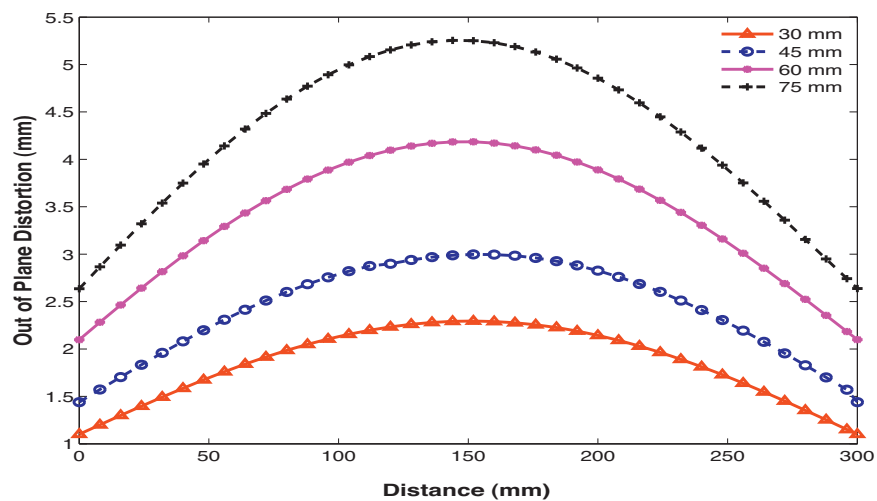


(b) Weld distortion along longitudinal direction
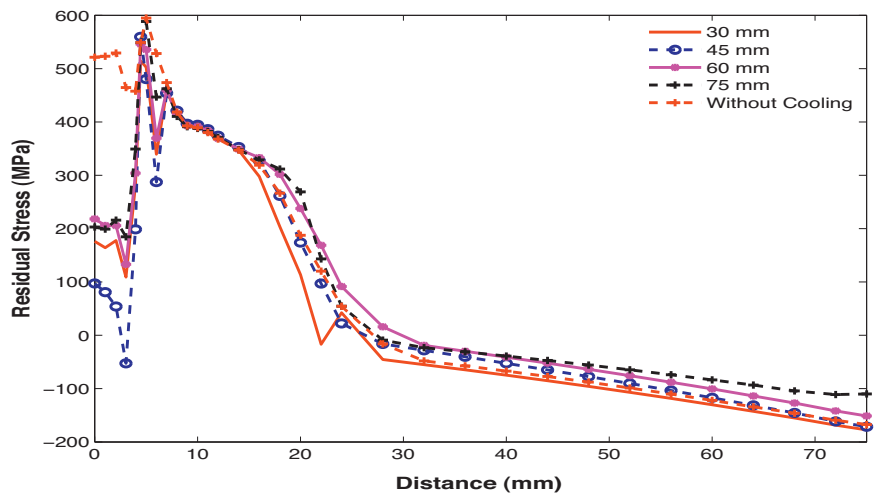


(c) Longitudinal residual stress

**Fig. 9.** Parametric study results.

distortion values with cooling are more than without cooling. Fig. 8(a) shows the longitudinal residual stress distribution in the transverse direction. The simulated results are nodal stress values of the nodes on the top surface of the plate mid-section. The

results clearly indicate that the welding with trailing heat sink has reduced stresses in the fusion zone and heat effected zone. However this change is not observed when analysis is done without phase transformation. The reduced stresses relaxes the geometry

and hence the distortions are higher in welding with cooling than conventional welding. In case of transverse residual stress plotted along width of the plate as shown in Fig. 8(b), no significant difference is observed between with and without cooling. The inset to Fig. 8(a) shows longitudinal stress contours which indicates tensile residual stresses near the weld line and compressive stresses at the free edge. It also shows the nature of out of plane distortion which is bending in the longitudinal direction and angular distortion in the direction perpendicular to the weld line.

## 5. Parametric study: distance between weld arc and cooling jet

The effect of distance between weld arc and trailing heat sink on temperature profile, distortion and residual stresses are studied numerically and results are plotted. The distance is varied in steps of 30 mm, 45 mm, 60 mm and 75 mm. Fig. 9(a) shows the truncation of temperature profile for different distances which increases the time gap between weld arc and heat sink.

Fig. 9(b) shows out of plane distortion measure in the longitudinal and transverse direction. They indicate that distortions increase with increased distance of cooling jet. With increased distance the cooling effect is reduced. Also, the final distortions depend on the weld pool size and shape which in turn depends on cooling rate. Fig. 9(c) shows longitudinal residual stress measured in the transverse direction. It shows lower stress values in the weld zone at a distance of 45 mm and effect is reduced for other cases. It would be desirable to have cooling jet as close as possible to the arc but practical constraints restrict this option with current experimental setup.

## 6. Conclusions

A two pass butt welding of 6 mm plate was simulated for conventional welding and welding with trailing heat sink. Experiments were conducted using LN2 as trailing heat sink. A parametric study was conducted by varying distance between weld torch and cooling jet. Based on this work the following conclusions are drawn:

- Longitudinal residual stresses significantly reduce in weld and fusion zone. However, distortions increase when welding was done with large distance of separation between heat sink and heat source.
- Distortion and residual stresses decrease when distance between weld torch and cooling jet was reduced.

### Acknowledgement

## References

Becker, M., Jordan, C., Lachhander, S.K., Mengel, A., Renauld, M., 2005. Prediction and Measurement of Phase Transformations, Phasedependent Properties and Residual Stresses in Steels. Lockheed Martin, Schenectady, NY, USA, Technical Report.

Borjesson, L., Lindgren, L.E., 2001. Simulation of multipass welding with simultaneous computation of material properties. Journal of Engineering Materials and Technology 123, 106–111.

Dai, H., Francis, J., Stone, H., Bhadeshia, H.K.D.H., Withers, P., 2008. Characterizing phase transformations and their effects on ferritic weld residual stresses with X-rays and neutrons. Metallurgical and Materials Transactions A 39A, 3070–3078.

Deng, D., 2009. FEM prediction of welding residual stress and distortion in carbon steel considering phase transformation effects. Materials and Design 30, 359–366.

Deng, D., Murakawa, H., 2008. Finite element analysis of temperature field, microstructure and residual stress in multi-pass butt-welded 2.25Cr 1Mo steel pipes. Computational Materials Science 43, 681–695.

Ferro, P., Porzner, H., Tiziani, A., Bonollo, F., 2006. The influence of phase transformations on residual stresses induced by the welding process 3D and 2D numerical models. Modelling and Simulation in Materials Science and Engineering 14, 117–136.

Goldak, J., Chakravarti, A., Bibby, M., 1984. A new finite element model for welding heat sources. Metallurgical Transactions B 15B, 299–305.

Han, Y.S., Lee, K., Han, M.S., Chang, H., Choi, K., Im, S., 2011. Finite element analysis of welding processes by way of hypoelasticity-based formulation. Journal of Engineering Materials and Technology 133, 1–13.

Heinze, C., Schwenk, C., Rethmeier, M., 2012. Numerical calculation of residual stress development of multi-pass gas metal arc welding under high restraint conditions. Materials and Design 35, 201–209.

Koistinen, D.P., Marburger, R.E., 1959. A general equation prescribing the extent of the austenite–martensite transformation in pure iron–carbon alloys and plain carbon steels. Acta Metallurgica 7, 59–60.

Leblond, J.B., Devaux, J., 1984. A new kinetic model for isothermal metallurgical tranformations in steels including effect of austenite grain size 32, 137–146.

Lee, C.H., Chang, K.H., 2009. Finite element simulation of the residual stresses in high strength carbon steel butt weld incorporating solid-state phase transformation. Computational Materials Science 46, 1014–1022.

Li, J., Guan, Q., Shi, Y., Guo, D., Du, Y., Sun, Y.C., 2004. Studies on characteristics of temperature field on GTAW with a trailing heat sink for titanium sheet. Journal of Materials Processing Technology 147, 328–355.

Soul, F.A., Yanhua, Z., 2005. Numerical study of the residual stress field during arc welding with a trailing heat sink. WIT Transactions on the Built Environment 84, 683–692.

Sudheesh, R.S., Siva Prasad, N., 2011. Finite element study of residual stresses and distortions in arc welding with a trailing liquid nitrogen heat sink. International Journal for Numerical Methods for Heat and Fluid Flow 21, 1050–1065.

Sysweld, 2005. Reference Manual. ESI Group, Paris.

van der Aa, E.M., Hermans, M., Richardson, I., van der Pers, N., Delhez, R., 2006a. Experimental study of the influence of a trailing heat sink on the welding residual stress distribution. Material Science Forum 524–525, 479–484.

van der Aa, E.M., Hermans, M.J.M., Richardson, I.M., 2006b. Conceptual model for stress and strain development during welding with trailing heat sink. Science and Technology of Welding and Joining 11 (4), 488–495.

Wang, L., Felicelli, S., 2007. Influence of proces parameters on the phase transformation and consequent hardness induced by the LENS process. Materials Processing Fundamentals, 63–72.

Yanagida, N., Koide, H., 2008. Reduction of residual stress in multi-layer welded plates by applying water shower cooling during welding. Journal of Solid Mechanics and Materials Engineering 2 (7), 943–954.